Four-dimensional dose reconstruction system for lung cancer VMAT treatment: a 4D phantom study

M. Hashimoto[1], Y. Ito[2], Y. Tanaka[3], M. Nakano[4*]

[1]School of Allied Health Sciences, Kitasato University, Sagamihara-shi, Kanagawa, Japan
[2]Radiation Oncology Department, Cancer Institute Hospital, Japanese Foundation for Cancer Research, Koto-ku, Tokyo, Japan
[3]Graduate School of Medical Sciences, Kitasato University, Sagamihara-shi, Kanagawa, Japan
[4]Department of Radiation Oncology, Kitasato University School of Medicine, Sagamihara-shi, Kanagawa, Japan

► *Original article*

ABSTRACT

Background: Recently, volumetric modulated arc therapy (VMAT) has been applied to the treatment of moving targets, such as lung tumors. The displacement of actual tumors during treatment based on an averaged four-dimensional (4D) planning computed tomography (CT) image set induces inconsistencies between dose distribution determined during the treatment planning step and the actual irradiated dose. The present study introduces a 4D dose reconstruction system and demonstrates its feasibility based on the results of dynamic thorax phantom experiments. **Materials and Methods:** Linear accelerator log files of two types—dynamic beam delivery log files and DynaLog files—were used to create the DICOM-RT Plan file with multiple-field irradiation. Dose distribution corresponding to each respiratory phase was calculated by planning the corresponding CT image set, and the accumulated dose distribution was subsequently reconstructed. In the experiment conducted in this study, two types of lung-tumor motion were considered—linear motion in the craniocaudal direction and combined motion in the craniocaudal and rotational directions. **Results:** The dose delivered to the center of a tumor was observed to vary by up to 4.4 %, depending on the initiation time of VMAT irradiation—the proposed system estimated the administered dose with an accuracy of 1.3 % or less. In the case of two-dimensional dose distribution, the pass rate of gamma analysis with a tolerance of 3 mm/3 % exceeded 96.6 %. **Conclusion:** The proposed system exhibited high dose-estimation accuracy for intricately moving targets, e.g., lung tumors, undergoing combined linear and rotational motion.

INTRODUCTION

Volumetric modulated arc therapy (VMAT) is an advanced irradiation technique that operates by continuously varying the rotational speed of a linear accelerator (linac) gantry, the dose rate, and the position of multi-leaf collimators (MLCs) [1,2]. It has been reported to exhibit several advantages over existing alternatives, e.g., short delivery duration and high conformity of dose delivery to the treatment targets[1,3,4] . It has been utilized for radiation treatment of various regions of the body, e.g., the prostate and the head-and-neck,[5–7] and even moving targets, e.g., lung tumors, where the dose distribution might be significantly affected by the magnitude of respiratory motion[8,9].

During VMAT treatment of lung tumors, internal target volumes (ITVs) are first delineated, and treatment plans are then created on an image set of slow-scan computed tomography (CT) or three-dimensional (3D) CT image sets prepared as an averaged image set of a four-dimensional (4D) CT series. An alternative technique utilizes mid-ventilation CT scans of the treatment target and conducts delineation as a time-averaged shape corresponding to each respiratory cycle[10]. The 4D treatment planning approach was proposed by Knopf *et al.*[11] However, in general, the dose delivered to the target and the dose distribution are evaluated using a 3D CT image set obtained by averaging an image set of 4D CT images,[12] as described above.

Based on the aforementioned discussion, it is clear that inconsistencies might be observed between the planned and delivered dose distributions in each treatment session because of the interplay of the non-synchronous motion of tumors and the leaves of the MLC unit[13–15]. The advance estimation of the magnitude of the difference between sessions is considerably difficult because of its complex dependence on the breathing cycle and motion of the linear accelerator gantry. Although some studies have argued that the prescribed dose can be delivered to

468

Int. J. Radiat. Res., Vol. 21 No. 3, July 2023

the planning target volume (PTV) at the end of a treatment series based on the averaging effect of dose distribution[16], it is highly important to evaluate the dose distribution of each treatment session as well as the accumulated dose distribution.

Dose reconstruction was proposed to evaluate the dose delivered to the target and the adjacent organs in a patient. Several approaches have been proposed to implement dose reconstruction, e.g., one based on the transit signal of photons through the patient observed using an electric portal imaging device (EPID) during actual treatment,[17] and another that re-calculates the dose distribution using treatment planning systems (TPSs) or Monte–Carlo simulations with linear accelerator log data, which contain the recorded mechanical motion of the linear accelerator during treatment. Recently, dose reconstruction was reportedly performed for a target undergoing respiratory motion using the latter method, and Poulsen *et al.* introduced a 4D dose reconstruction method to calculate dose distribution on TPS by considering 4D tumor motion and mechanical motion of the linac[18]. They proposed displacing the isocenter in the TPS environment depending on the location of the tumor, which exhibited motion only in the craniocaudal direction, and obtained consistent results based on the measurements.

The primary purpose of this study was to develop a system to reconstruct 4D dose distributions using the approach proposed by Poulsen *et al.*[18] and demonstrate its feasibility in the case of VMAT treatment for lung cancer. First, TPS was used to reconstruct the dose distribution based on DICOM-RT plans and 4D CT image sets corresponding to each respiratory phase. The DICOM-RT plans were created using linac log data acquired during the treatment session, and the respiratory phase at each moment was identified using a real-time position management (RPM) system that was run during the treatment session. Then, dose calculation was performed on the planning 4D CT of the identified phase corresponding to each control point. The accuracy of the reconstructed dose distribution was evaluated using VMAT treatment plans for lung tumors exhibiting two types of movement-only in the craniocaudal direction and in both craniocaudal and rotational directions. The present method differs from conventional methods in that it enables dose reconstruction that takes into account three-dimensional positional changes in tissues and organs during irradiation, i.e., the variation of transmission length from the body surface to the target due to respiratory motion. In this study, we demonstrate for the first time how to construct a 4D dose distribution reconstruction system and how to evaluate its accuracy including the interplay effect using dynamic thorax phantom, which can simulate 3D tumor motion.

MATERIALS AND METHODS

Dose reconstruction system

The dose reconstruction process introduced in this study consisted of three primary portions-generation of a DICOM treatment plan (RT Plan) file with multiple irradiation fields to imitate irradiated VMAT treatment, correlation of each irradiation field to the corresponding respiratory phase, and dose calculation and accumulation using TPS. The general workflow of the proposed system is depicted in figure 1. The system required three types of input data-log data files of a linear accelerator, respiratory waveforms, and cine-image series captured using an EPID detector—acquired during the actual treatment session. In the present study, these data were acquired using a CLINAC 21EX linear accelerator, RPM system, an aS1000 EPID detector provided by Varian Medical Systems (Palo Alto, CA, USA). Log data files were used to generate a DICOM RT Plan file with an identical number of irradiation fields compared to the control points of the original RT Plan file. Respiratory waveform data from the RPM and EPID cine-image series were used to correlate the gantry angles used in the actual treatment session with corresponding respiratory phases. Dose reconstruction was performed on the 4D CT image set using an Eclipse (Varian Medical Systems, Palo Alto, CA, USA) TPS after considering the respiratory phases and actual gantry angles. Each subprocess of the proposed system is described in further detail in the following subsections.
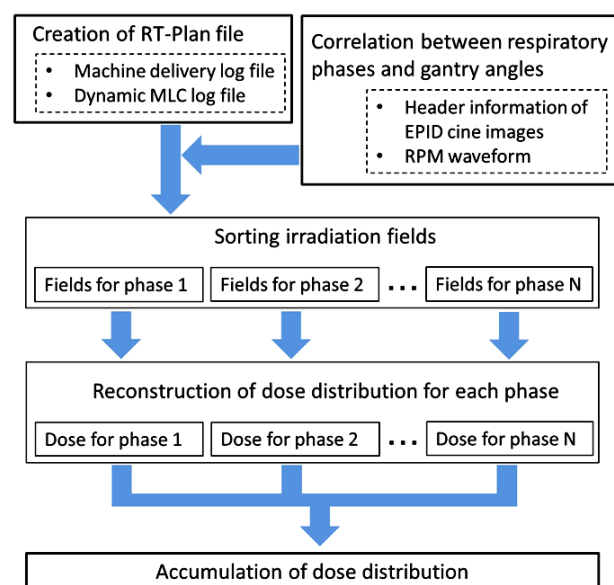

Figure 1. Workflow of 4D dose reconstruction system introduced in the present study.

Generation of DICOM RT Plan file with multiple-field irradiation

Dose calculation was performed on the TPS by converting the actual motion of the linear accelerator recorded in the log data files into a multiple-field

DICOM RT Plan file using an in-house software written in C++. The number of irradiation fields presents in the generated RT plan file was identical to the number of control points in the original RT plan file, and the gantry angle of each irradiation field in the RT Plan file was equal to that of the corresponding control point. Machine-delivery and dynamic MLC log files were used in this study; in particular, the former recorded monitor units (MUs) corresponding to each irradiation angle and discretized gantry-angle values, and the latter included the positions of the MLC leaves, angle of the collimator unit, positions of the jaws, and corresponding gantry angles as discrete values. The gantry angles recorded in the log files were not consistent with the angles of the control points; therefore, the MUs for all irradiation angles were converted into MUs for control points via linear interpolation. The same process was repeated for the positions of the MLCs and jaws, and the collimator angle.

Assignment of control points to corresponding respiratory phases

The generated RT Plan file described in Section II.A.1 contained 178 irradiation fields, which was equivalent to one arc of VMAT irradiation with a rotation angle of 358°. The system introduced in this study reproduced the correlation between actual gantry angles and respiratory phases during treatment sessions using respiratory waveforms obtained from the RPM system and the EPID cine-image series.

The RPM system, which automatically detected the position of the infrared reflective marker block, enabled the detection and storage of temporal variation of chest wall displacement from an initial status as respiratory waveform data. During the experimental part of this study, the waveform contained correlated information between the position of the chest wall, which corresponded to the position of the marker block on the surrogate platform of the dynamic thorax phantom described in Section II.B, and the time elapsed from the beginning of irradiation. An EPID cine-image series was also acquired during irradiation, which recorded the correlation between the gantry angle and the elapsed time as the DICOM header information of the image series. Then, the respiratory waveform and gantry angle transition were correlated with the elapsed time.

The aforementioned RT Plan file with the multiple irradiation fields was divided into as many RT Plan files as the number of respiratory phases of 4D CT acquisition mentioned in Section II.B.1. This division was performed using an in-house software written in C++.

Dose calculation on the TPS

The dose distribution was calculated using Eclipse TPS based on the DICOM RT Plan files, after categorizing them in terms of respiratory phases and importing them into the TPS, and the correlation information between each pair of respiratory phase and gantry angle. In this study, the anisotropic analytical algorithm was chosen for dose calculation with a grid size of 2.5×2.5 mm^2 and a planning CT image series slice thickness of 2.5 mm. Dose-distribution reconstruction was performed using imported RT Plan files on the CT image set of each respiratory phase. The evaluation was also implemented for the accumulated dose distribution, including all 20 phases considering both types pf motion. The dose distribution was first calculated for each respiratory phase and exported as DICOM RT-Dose files. Subsequently, the dose distributions of all respiratory phases were accumulated by exactly aligning their three-dimensional positions and angles to the inhalation phase.

Phantom experiments

The accuracy of the 4D dose reconstruction system was evaluated by comparing its results with actual measurements recorded using a dynamic thorax phantom. The measurements were performed by simulating various respiratory patterns using a dynamic thorax phantom model 008A (CIRS, Norfolk, VA, USA), as depicted in figure 2 (a). Two types of moving sections were considered in this study- ionization chamber insertion and film insertion (figure 2 (b)). The moving section having ionization chamber insertion was one of the accessories of CIRS dynamic phantom, and the film insertion was a custom-made product made up of materials provided by Kyoto Kagaku Co., Ltd. (Kyoto, Japan). Both the moving sections were made by Tough-Lung phantom and included a simulated tumor with a diameter of 3 cm made by the Tough-Water phantom. A reflective marker for the infrared tracking camera of the RPM system was placed on the surrogate platform of the phantom. Lung tumors have been reported to move not only in the craniocaudal direction, but also in the left-right (LR) and anterior-posterior (AP) directions [19,20]. The dynamic thorax phantom enabled the performance of combined motion in the craniocaudal and rotational directions. The motion of the reflection marker was synchronized with that of the tumor phantom. In the tumor section, the position of the tumor was off-centered by 1.25 cm, as depicted in figure 2(b), and the two types of motion were considered—craniocaudal linear motion and twisted motion combining craniocaudal and rotational motions. The amplitude of the craniocaudal motion was taken to be 10 mm (20 mm peak-to-peak), and the angle of rotational motion was 45°.

Acquisition of the 4D CT image series

Two types of tumor motion—linear motion only in the craniocaudal direction and combined linear and rotational (45°) were performed using a dynamic

thorax phantom, and 4D CT images were acquired using a Discovery PET/CT 600 system (GE Healthcare, Waukesha, WI, USA). The thickness of the CT image was 2.5 mm and respiratory motion was recorded during CT scans using the RPM system with an infrared reflecting marker. CT image sets corresponding to 20 respiratory phases were reconstructed.
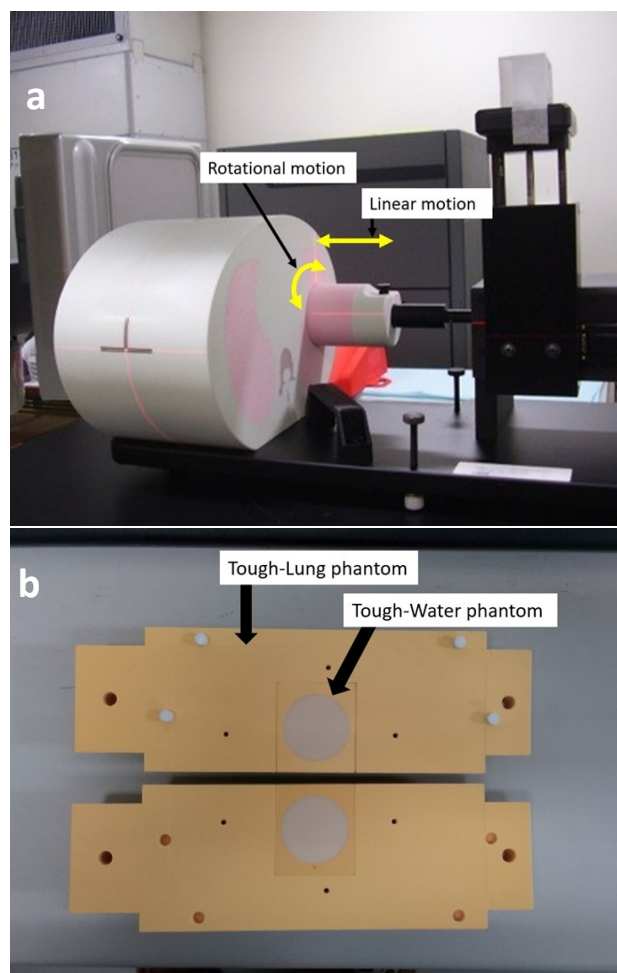

Figure 2. CIRS dynamic thorax phantom: **(a)** whole phantom configuration on the patient couch and **(b)** the moving section for film measurement fabricated using lung equivalent and water equivalent materials.
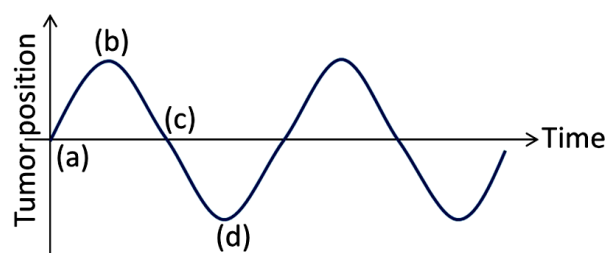
II.B.2 Treatment planning

The original treatment plans were based on an averaged 4D CT image set. The ITV was delineated in terms of the volume of the tumor merged over all respiratory phases, and the PTV was defined as the ITV with a 10 mm margin in three dimensions. The organs-at-risk (OARs), such as the heart, spinal cord, left and right lungs, and esophagus, were also delineated and accounted for in the optimization calculation of TPS, with constrained rules in the author's institution. The created VMAT plans totaled to 2.0 Gy per fraction and comprised two arcs of a 6 MV photon beam with a maximum dose rate of 600 MU/min. The dose reconstruction system proposed in this study was capable of calculating the dose distribution including two arcs simultaneously, but we performed the evaluation for each arc separately to avoid the dose averaging effect.

II.B.3 Dynamic thorax phantom experiments using ionization chamber and radiographic film

The measurements were implemented for the two treatment plans mentioned in Section II.B.2 using an ionization chamber and radiographic films. The ionization chamber was placed at the center of the target, and the absorbed doses and dose distributions on the cross-section of the moving section were measured using radiographic films. The RPM system and EPID cine image series with a frame rate of 10 frames per second (fps) were also measured during the irradiation sessions, as mentioned in Section II.A.2. For each plan, four measurements were recorded at different times to observe the impact of the interplay effect. Figures 3(a)–(d) depict four different timings of irradiation commencement. Two types of experiments were conducted, as described below.

Figure 3. Initiation times for irradiation and corresponding tumor positions. The position (b) indicates the exhale phase and (d) indicates the inhale phase.

(a) Ionization chamber

The absolute dose administered to the target was measured by inserting a PTW model 31016 microchamber detector (PTW Freiburg GmbH, Freiburg, Germany) into the center of the target in the moving solid epoxy phantom in the dynamic thorax phantom. The chambers were cross-calibrated using a PTW Farmer chamber model 30013 with a sensitive volume of 0.6 cm^3, which was calibrated by the Japanese primary standard dosimetry laboratory. The beam quality factor, k_Q, was determined based on the JSMP12 dosimetry protocol.[21] The absorbed dose was obtained by multiplying the two aforementioned factors by the measured amount of ionization. Correction factors—such as the ion recombination correction factor, k_s, and polarity effect correction factor, k_{pol}—were calculated based on advance measurements and were applied to the measured amounts of ionization. The correction factor for temperature and pressure, k_{TP}, was also utilized. The RAMTEC 1000 Plus (TOYO MEDIC Co., Ltd., Tokyo, Japan) electrometer was used for the measurement.

(b) Film measurement and readout

6.1 × 13.3 cm^2 film pieces of EDR2 (Carestream

Health Inc., Rochester, NY, USA) were inserted into the solid epoxy phantom within the dynamic thorax phantom. They were left for 24 hours after irradiation for self-development.[22–24] The irradiated film pieces were scanned using ES-10000G (Seiko Epson Corp., Nagano, Japan) with a resolution of 150 dpi in 16-bit grayscale, and the scanned images were saved in tagged image file format. The dose response curve of the EDR2 film was estimated in advance using a 30 cm-long square-shaped Tough-Water phantom (Kyoto Kagaku Co. Ltd., Kyoto, Japan). The phantom was piled up to a height of 30 cm and a source-to-surface distance (SSD) of 90 cm was implemented. The films were irradiated at a depth of 10 cm from the upper surface, and the irradiated MUs were measured between 25 and 325 MU at intervals of 25 MU.

II.B.4 Dose reconstruction using the proposed system

The implementation of dose reconstruction using the proposed system during irradiation sessions is described in Section II.B.3. It was performed using the header information of EPID cine images, RPM waveform, and contents of log files, which were acquired during the irradiation sessions. The reconstructed dose at the center of the tumor and the overall dose distribution were compared with the measurements of the ionization chamber and films.

II.C. Statistical analysis

The reconstructed and measured dose distributions were compared and analyzed in terms of the gamma index using Simple IMRT Analysis software Ver. 1.0 (Triangle Products, Kashiwa-shi, Chiba, Japan) considering a criterion of 3 mm/3%.

RESULTS

III.1 Comparison of doses administered to the center of tumor

Table 1 presents a comparison between the measured and reconstructed doses at the center of the tumor corresponding to linear motion, and combined linear and rotational motion. In the case of linear motion, a maximum difference of 4.4 % was observed, depending on the initiation time of irradiation, whereas in the case of combined motion, a maximum difference of 3.2 % was observed. These differences were attributed to the interplay effect, and the proposed system was able to estimate the irradiated dose with a maximum difference of 1.3 %, even in the presence of the interplay effect.

III.2 Comparison of dose distributions

The dose distribution obtained using the proposed system was compared with the film measurement results, as depicted in figure 4(a)–(d). Table 2 records the pass rate of the gamma-analysis results with a tolerance of 3 mm/3%, which was calculated within the area corresponding to doses exceeding 30 % of the prescribed dosage. Although different dose distributions were observed depending on the initiation time of irradiation, as depicted in figure 4, the isodose curves of the measurement and reconstruction exhibited good agreement. The obtained pass rate of the gamma analysis was greater than 96 % corresponding to all measurements. Relatively larger inconsistencies were observed in figure 4(c) and (d), which could be caused by consideration of combined linear and rotational motion. figure 4 reveals that the direction of blurring of the measured dose was in the vertical direction (i.e., craniocaudal direction) in (a) and (b), and in both the vertical and lateral directions in (c) and (d), which were the cases of combined linear and rotational motion. The results indicate that although differences were observed between dose distributions depending on the initiation time of irradiation, the proposed system reconstructed the dose distribution of actual irradiation sessions with an accuracy that cannot be achieved via treatment simulation using a treatment planning system.

Table 1. Dose measurement results obtained by inserting PTW 31016 micro-chamber into the moving section of CIRS dynamic thorax phantom

Type of motion		Linear			Linear + Rotational		
Start position		Calculated dose [Gy]	Measured dose [Gy]	Error [%]	Calculated dose [Gy]	Measured dose [Gy]	Error [%]
Dose	(a)	1.797	1.799	−0.1%	1.701	1.706	−0.3%
	(b)	1.712	1.724	−0.7%	1.644	1.653	−0.5%
	(c)	1.725	1.748	−1.3%	1.653	1.672	−1.1%
	(d)	1.785	1.780	0.3%	1.665	1.672	−0.4%
Relative values normalized by (b)	(a)	105.0%	104.4%		103.5%	103.2%	
	(b)	100.0%	100.0%		100.0%	100.0%	
	(c)	100.8%	101.4%		100.5%	101.1%	
	(d)	104.3%	103.2%		101.3%	101.1%	

Table 2. Gamma analysis results with tolerance of 3 mm/3 % for linear motion and combined linear and rotational motion of tumor phantom obtained using EDR2 radiographic film.

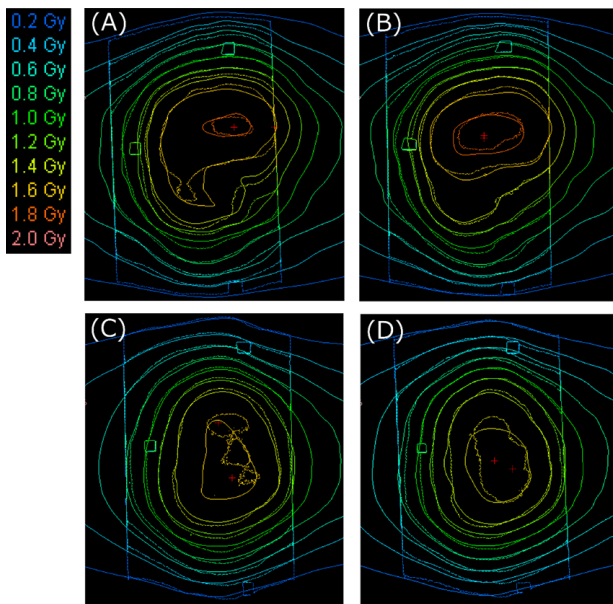| Type of motion	Start position	Gamma pass rate [%]
Linear	(a)	96.6
	(d)	98.9
Linear + Rotational	(a)	97.2
	(d)	97.6

Figure 4. Dose distribution measured using EDR2 film: **(A)** linear motion starting at position (a), **(B)** linear motion starting at position (d), **(C)** linear and rotational motion starting at position (a), and **(D)** linear and rotational motion starting at position (d). Solid and dotted lines represent reconstructed and measured doses, respectively.

DISCUSSION

The experimental results demonstrated that the error of the reconstructed dose obtained using the proposed dose reconstruction system with respect to the measured dose was less than 1.3 % at the center of the tumor. Because the proposed system discretizes the position of the tumor to several different positions owing to the use of the 4D CT image reconstruction technique, the error between the measured and reconstructed doses is expected to decrease as the magnitude of tumor motion in each discretized phase is decreased. Thus, it is possible to further reduce the error by dividing the tumor motion into a greater number of phases. In the phantom experiments conducted in this study, the peak-to-peak amplitude of the tumor motion was taken to be 20 mm, which was larger than the typical amplitude of lung-tumor motion. Although the actual error may be lower than 1.3 % in the case of real patients, peak-to-peak tumor motion amplitudes exceeding 20 mm may induce larger errors. Therefore, an error assessment of the dose reconstruction accuracy with respect to the magnitude of tumor motion and the number of discretized respiratory phases must be conducted in a future work.

The gamma analysis results obtained by Poulsen *et al.*[18] in the case involving only linear motion in the CC direction exhibited a pass rate of 99 % with a tolerance of 2 mm/2%, whereas the pass rate in the present study ranged from 97.2 % to 98.9 % with a tolerance of 3 mm/3%; thus, close agreement was observed. The difference between the study by Poulsen *et al.* and the present study is the consideration of the complexity of tumor motion and the effect of discretization mentioned above. Film measurements indicated that the degree of blurring of the dose distribution might be affected by the type of motion, and that combined craniocaudal and rotational motion might induce blurring in both the longitudinal and vertical directions. Lin et al. reported a method to implement patient-specific QA with dose calculation in the treatment planning system using fluence maps obtained by EPID cine images and considering time variation of irradiated dose.[31] In this report, the clinical SBRT plans using 3D-CRT and IMRT fields were irradiated for uniaxial motion phantom of 1.1 cm amplitude and 4 seconds period, and the results were compared with those of a cylindrical diode array detector (ArcCheck system, Sun Nuclear, Inc., Melbourne, FL, USA). The resulting dose reconstruction accuracy was more than 97.6% of the gamma pass rate (2% / 2 mm) considering the temporal information. In this method, the EPID detects signals after transmission through the phantom or patient; therefore, it is necessary to remove the effects of dose attenuation and scattered radiation due to the phantom and patients themselves to obtain the incident fluence map required for dose calculation and to correct the dose using the MU values for each moment in one irradiation session. Therefore, performing accurate correction is highly complicated. In addition, when performing dose reconstruction on a real patient, the EPID must be opened and located in the imaging position while the treatment is being performed, which requires other considerations, such as collisions of the EPID panel with the couch or patients. Recently, A. Meijers et al. reported a method for reconstructing 4D dose distributions in proton therapy using a method similar to that of the present study[32], and it also supports the validity of our method, which aims to assess the actual dose to the patient considering the interplay effect.

The results of the reconstructed dose distribution exhibited good agreement with the measured distribution obtained using the EDR2 film. We employed a dynamic thorax phantom with a solid tumor section that followed a predetermined trajectory—this enabled the accumulation of dose distribution without considering deformation. However, in real-world cases, the shape of the tumor might deform adjacent organs as well, and deformable registration should be used to accumulate dose distribution. Moreover, errors may be induced by the deformable registration technique.[28, 29, 30] Although the errors induced by differences between deformation algorithms are not negligible in the proposed method, deformable registration and accumulation using this method were not considered

in this study. Instead of accumulating the dose distribution with some errors, the proposed system enabled the independent evaluation of the dose distribution corresponding to each respiratory phase during the process. Independent dose evaluation of each respiratory phase without accumulation is expected to aid precise dose distribution evaluation. Such evaluation methods should be developed in future works.

In the proposed system, EPID cine images were acquired during irradiation solely to obtain records of the gantry angle. Thus, it can be simply replaced by attaching a gantry angle sensor to the gantry, and EPID cine images could be potentially used for tumor position detection and respiratory phase recognition. Cine images acquired by a kV OBI unit mounted perpendicular to the treatment beam on the linear accelerator gantry is another viable option.[27] Although, in this study, the sole purpose of EPID cine images was to record gantry angles, cine image acquisition can also be used for the detection of tumor positions. This is expected to enable the application of the proposed system to clinical sites without RPM systems. The tumor position detection function is expected to be an interesting topic for future research.

In this study, dose reconstruction was performed using a 4D CT image series, which was also used during the treatment planning step. It enabled reconstruction of the dose distribution of lung tumors and surrounding lung regions undergoing complex motion. Previously conducted studies required displacement of the body and OAR contours in the L-R and A-P directions for accumulated dose reconstruction [18]—this is redundant in the proposed system. The intrafractional repeatability of lung tumor trajectory may be problematic in this context; for example, the migration of the tumor location at the moment of max-inhalation or max-exhalation during the actual irradiation session might induce errors in dose reconstruction results. The use of the 4D cone-beam CT (CBCT) image series is expected to minimize such errors. Dose reconstruction on pre-treatment or in-treatment 4D CBCT image sets is a good option to minimize interfractional positional errors and consider the change in tumor size from the perspective of adaptive radiotherapy (ART). Although the use of 4D CBCT still involves drawbacks owing to its pixel value inaccuracy, the overall accuracy of dose reconstruction results can be expected to be improved by considering precise tumor positions on in-treatment 4D CBCT image sets. [25,26]

The present study demonstrates the feasibility of 4D dose calculations using a 4D thorax phantom containing a moving lung tumor module. The proposed method may be applied not only for lung tumors but also for tumors located in the upper abdominal area that are be affected by respiratory motion.

CONCLUSIONS

The present study introduced a 4D dose reconstruction system that accounts for the actual motion of a lung tumor in both the craniocaudal and rotational directions and the motion of a linear accelerator. The results obtained from phantom-based experiments revealed good agreement between the reconstructed and measured doses-the reconstructed dose at the center of the target was within ± 2% of the measured dose, and the pass rate of gamma analysis exceeded 90 % corresponding to each measurement. The present study enabled the determination of the actual irradiated dose to the target, and we believe that the proposed system will contribute to the successful implementation of ART in clinical situations.

REFERENCES

1. Otto K (2008) Volumetric modulated arc therapy: IMRT in a single gantry arc. *Med Phys*, *35(1)*: 310-317.
2. Palma DA, Verbakel WFAR, Otto K, Senan S (2010) New developments in arc radiation therapy: a review. *Cancer Treat Rev*, *36(5)*: 393-399.
3. Teoh M, Clark CH, Wood K, Whitaker S, Nisbet A (2011) Volumetric modulated arc therapy: a review of current literature and clinical use in practice. *Br J Radiol*, *84*: 976-996.
4. Bedford JL (2009) Treatment planning for volumetric modulated arc therapy. *Med Phys*, *36(11)*: 5128-5138.
5. Pesce GA, Clivio A, Cozzi L, Nicolini G, Richetti A, Salati E, *et al.* (2010) Early clinical experience of radiotherapy of prostate cancer with volumetric modulated arc therapy. *Radiat Oncol*, *5(1)*: 54.
6. Holt A, Van Gestel D, Arends MP, Korevaar EW, Schuring D, Kunze-Busch MC, *et al.* (2013) Multi-institutional comparison of volumetric modulated arc therapy vs. intensity-modulated radiation therapy for head-and-neck cancer: a planning study. *Radiat Oncol*, *8(1)*: 26.
7. Verbakel WFAR, Cuijpers JP, Hoffmans D, Bieker M, Slotman BJ, Senan S (2009) Volumetric intensity-modulated arc therapy vs. conventional IMRT in head-and-neck cancer: a comparative plan-

ning and dosimetric study. *Int J Radiat Oncol Biol Phys*, **74(1)**: 252 -259.

8. Holt A, van Vliet-Vroegindeweij C, Mans A, Belderbos JS, Damen EMF (2011) Volumetric-modulated arc therapy for stereotactic body radiotherapy of lung tumors: a comparison with intensity-modulated radiotherapy techniques. *Int J Radiat Oncol Biol Phys*, **81(5)**: 1560-1567.

9. Navarria P, Ascolese AM, Mancosu P, Alongi F, Clerici E, Tozzi A, *et al*. (2013) Volumetric modulated arc therapy with flattening filter free (FFF) beams for stereotactic body radiation therapy (SBRT) in patients with medically inoperable early stage non small cell lung cancer (NSCLC). *Radiother Oncol*, **107(3)**: 414-418.

10. Wolthaus JWH, Schneider C, Sonke J-J, van Herk M, Belderbos JSA, Rossi MMG, *et al*. (2006) Mid-ventilation CT scan construction from four-dimensional respiration-correlated CT scans for radiotherapy planning of lung cancer patients. *Int J Radiat Oncol*, **65(5)**: 1560-1571.

11. Knopf A, Nill S, Yohannes I, Graeff C, Dowdell S, Kurz C, et al. (2014) Challenges of radiotherapy: Report on the 4D treatment planning workshop 2013. *Phys Medica*, **30(7)**: 809-815.

12. Huang L, Park K, Boike T, Lee P, Papiez L, Solberg T, *et al*. (2010) A study on the dosimetric accuracy of treatment planning for stereotactic body radiation therapy of lung cancer using average and maximum intensity projection images. *Radiother Oncol*, **96(1)**: 48-54.

13. Berbeco RI, Pope CJ, Jiang SB. Measurement of the interplay effect in lung IMRT treatment using EDR2 films. *J Appl Clin Med Phys*, **7(4)**: 33-42.

14. Ong C, Verbakel WFAR, Cuijpers JP, Slotman BJ, Senan S (2011) Dosimetric Impact of Interplay Effect on RapidArc Lung Stereotactic Treatment Delivery. *Int J Radiat Oncol*, **79(1)**: 305-311.

15. Rao M, Wu J, Cao D, Wong T, Mehta V, Shepard D, *et al*. (2012) Dosimetric impact of breathing motion in lung stereotactic body radiotherapy treatment using image-modulated radiotherapy and volumetric modulated arc therapy. *Int J Radiat Oncol Biol Phys*, **83 (2)**: e251-e256.

16. Stambaugh C, Nelms BE, Dilling T, Stevens C, Latifi K, Zhang G, *et al.* (2013) Experimentally studied dynamic dose interplay does not meaningfully affect target dose in VMAT SBRT lung treatments. *Med Phys*, **40(9)**: 91710.

17. van Zijtveld M, Dirkx MLP, de Boer HCJ, Heijmen BJM (2007) 3D dose reconstruction for clinical evaluation of IMRT pretreatment verification with an EPID. *Radiother Oncol*, **82(2)**: 201-207.

18. Poulsen PR, Schmidt ML, Keall P, Worm ES, Fledelius W, Hoffmann L (2012) A method of dose reconstruction for moving targets compatible with dynamic treatments. *Med Phys*, **39(10)**: 6237-6246.

19. Nakagawa K, Haga A, Kida S, Masutani Y, Yamashita H, Takahashi W, *et al*. (2013) 4D registration and 4D verification of lung tumor position for stereotactic volumetric modulated arc therapy using respiratory-correlated cone-beam CT. *J Radiat Res*, **54(1)**: 152-156.

20. Nakagawa K, Haga A, Sasaki K, Kida S, Masutani Y, Yamashita H, *et al*. (2014) Lung tumor motion reproducibility for five patients who received four-fraction VMAT stereotactic ablative body radiotherapy under constrained breathing conditions: a preliminary study. *J Radiat Res*, **55(6)**: 1199-1201.

21. Saitoh H (2013) Advance in dose standard and dosimetry protocol for external beam radiation therapy. *Igaku Butsuri*, **33(suppl.2)**: 1-12.

22. Childress NL, Rosen II (2004) Effect of processing time delay on the dose response of Kodak EDR2 film. *Med Phys*, **31(8)**: 2284.

23. Childress NL, Salehpour M, Dong L, Bloch C, White RA, Rosen II (2005) Dosimetric accuracy of Kodak EDR2 film for IMRT verifications. *Med Phys*, **32(2)**: 539.

24. Shi C, Papanikolaou N, Yan Y, Weng X, Jiang H (2006) Analysis of the sources of uncertainty for EDR2 film-based IMRT quality assurance. *J Appl Clin Med Phys*, **7(2)**: 1-8.

25. Lee L, Le QT, Xing L (2008) Retrospective IMRT Dose Reconstruction Based on Cone-Beam CT and MLC Log-File. *Int J Radiat Oncol Biol Phys*, **70(2)**: 634-644.

26. van Zijtveld M, Dirkx M, Heijmen B (2007) Correction of conebeam CT values using a planning CT for derivation of the "dose of the day." *Radiother Oncol*, **85(2)**: 195-200.

27. Kida S, Masutani Y, Yamashita H, Imae T, Matsuura T, Saotome N, *et al.* (2012) In-treatment 4D cone-beam CT with image-based respiratory phase recognition. *Radiol Phys Technol*, **5(2)**: 138-147.

28 Nenoff L, Ribeiro CO, Matter M, Hafner L, Josipovic M, Langendijk JA, *et al.* (2020) Deformable image registration uncertainty for inter-fractional dose accumulation of lung cancer proton therapy. *Radiother Oncol*, **147**: 178-185.

29 Lowther NJ, Marsh SH, Louwe RJW (2020) Quantifying the dose accumulation uncertainty after deformable image registration in head-and-neck radiotherapy. *Radiother Oncol*, **143**: 117-125.

30 Bai X, Wang B, Wang S, Wu Z, Gou C, Hou Q (2020) Radiotherapy dose distribution prediction for breast cancer using deformable image registration. *Biomed Eng Online* **19(1)**: 3.

31 Lin MH, Li J, Wang L, Koren S, Fan J, Forkal E, Ma CM (2012) 4D patient dose reconstruction using online measured EPID cine images for lung SBRT treatment validation. *Med Phys*, **39(10)**: 5949-5958.

32 Meijers A, Knopf AC, Crijns AP, Ubbels JF, Niezink AG, Langendijk JA, *et al.* (2020) Evaluation of interplay and organ motion effects by means of 4D dose reconstruction and accumulation. *Radiother Oncol*, **150**: 268-274.